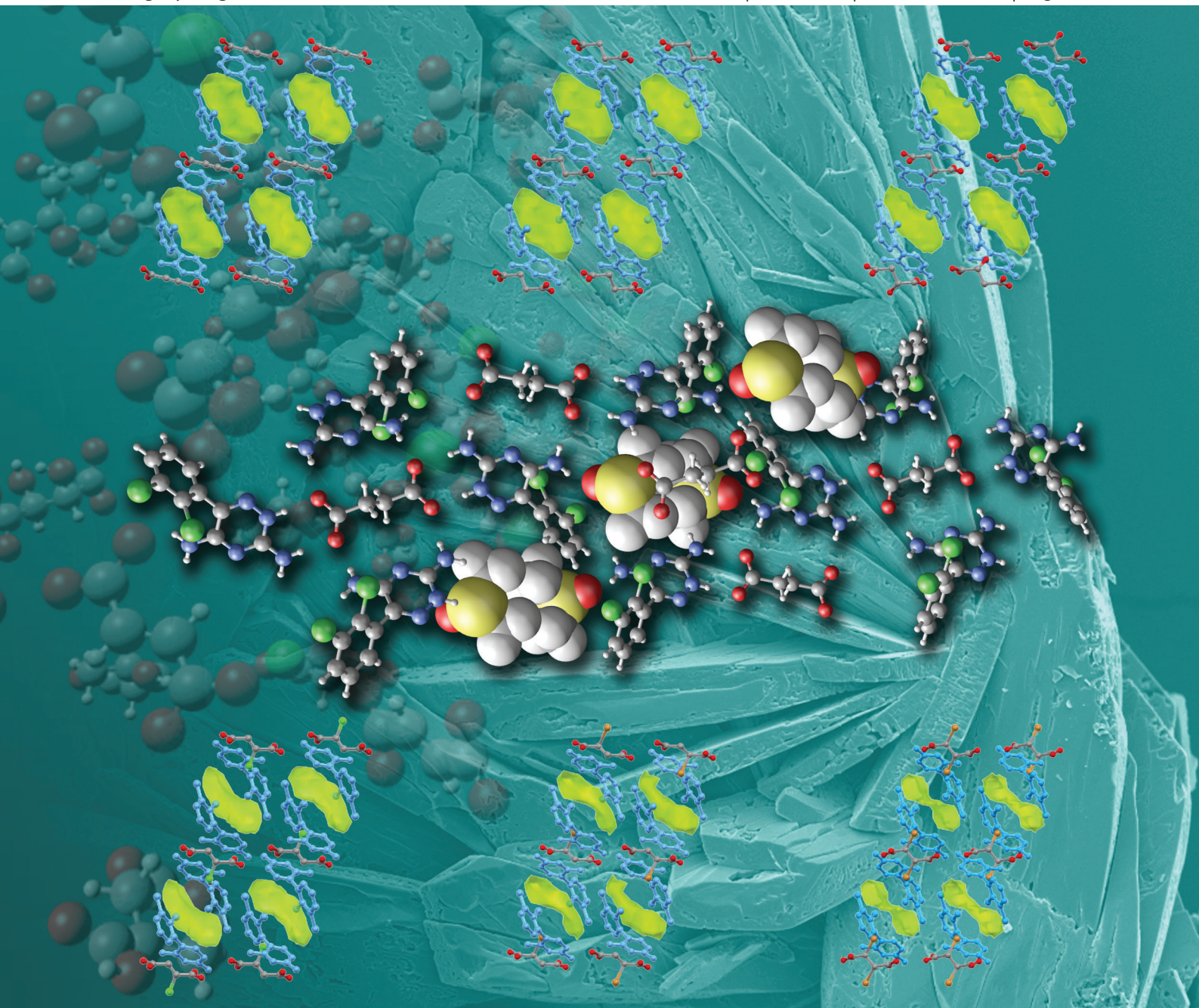


# CrystEngComm

[www.rsc.org/crystengcomm](http://www.rsc.org/crystengcomm)

Volume 14 | Number 23 | 7 December 2012 | Pages 7809–8302



RSC Publishing

**COVER ARTICLE**

Galcera, Jones *et al.*  
Isostructural organic binary-host frameworks with tuneable and diversely decorated inclusion cavities

Cite this: *CrystEngComm*, 2012, 14, 7898–7906

www.rsc.org/crystengcomm

PAPER

## Isostructural organic binary-host frameworks with tuneable and diversely decorated inclusion cavities†

Judit Galcera,<sup>\*ab</sup> Tomislav Friščić,<sup>b</sup> Katarzyna E. Hejczyk,<sup>b</sup> László Fábián,<sup>c</sup> Stuart M. Clarke,<sup>b</sup> Graeme M. Day,<sup>b</sup> Elies Molins<sup>a</sup> and William Jones<sup>\*b</sup>

Received 13th April 2012, Accepted 6th July 2012

DOI: 10.1039/c2ce25550b

The search for materials capable of storing small molecular species is experiencing a shift from solids with permanent porosity towards organic materials capable of the uptake and release of low-molecular-weight guests. We demonstrate that a solid mixture of the pharmaceutical compound lamotrigine with a range of saturated and unsaturated 1,4-butanedicarboxylic acids, when in combination with a third molecule, can result in the formation of a family of isostructural materials involving a structurally persistent binary-host framework based on a hydrogen-bonded molecular salt of lamotrigine and the acid. A systematic study, based on mechanochemical screening, has revealed a remarkable robustness to subtle changes in the chemical functionality of the acid in that at least 12 different acids can be used in combination with lamotrigine to generate isostructural binary-host frameworks. Such robust isostructurality results in the important attribute that the shape, size and surface chemistry of the inclusion cavities can be fine-tuned by systematic variation of the substituents on the dicarboxylic acid.

### Introduction

Supramolecular synthesis and molecular self-assembly<sup>1–3</sup> are increasingly versatile and attractive approaches for the construction of functional materials.<sup>4</sup> Particular success has been demonstrated in using metal-ligand coordination bonds for the design of materials for molecular inclusion<sup>5–8</sup> in hosts with permanent porosity.<sup>9–11</sup> An alternative to coordination bonds is the utilization of directional non-covalent interactions (based on organic molecular constituents), such as hydrogen<sup>12</sup> or halogen bonds,<sup>13</sup> and the incorporation of robust supramolecular synthons.<sup>3,14</sup> This approach has the important inherent advantage that, in principle, it allows the use only of organic components for the construction of low-molecular-weight materials for molecular inclusion. Whereas the synthon-based approach is remarkably successful in the synthesis of multi-component crystals with applications as pharmaceutical materials,<sup>15–18</sup> reliable strategies for molecular inclusion using modular binary-host materials remain a challenge.<sup>19–24</sup> While inclusion framework structures might sometimes be predictable,<sup>25,26</sup> the challenge of their design is related, in part,

to the relative weakness of the underlying interactions hindering the formation of permanently porous structures. As a result, the design of organic inclusion materials is expected to rely on dynamic structures<sup>27,28</sup> which, while not porous themselves, can rearrange to achieve selective molecular inclusion in the presence of suitable guests. So far, the most successful multi-component pure organic solids for molecular inclusion are those based on charged-assisted hydrogen bonds, which are strengthened through Coulombic attractions.<sup>27</sup> Notably, Ward and co-workers have demonstrated that guanidinium sulfonates readily act as binary-hosts for molecular inclusion.<sup>29–31</sup> In these systems the host structure is based on a common persistent two-dimensional hydrogen-bonded network structure formed between guanidinium and sulfonate ions.<sup>32</sup> The layered nature of this self-assembled structure permits structural variability in the third dimension and, consequently, guanidinium sulfonate hosts are able to adapt to large variations in guest size and shape.<sup>33</sup>

Isostructural solids are defined as solids that have different chemical compositions and identical or very similar crystallographic parameters and molecular packing motifs.<sup>34,35</sup> Isostructurality has recently been proposed as an alternative basis for the controlled construction of functional molecular materials,<sup>36–38</sup> since the concept allows different molecular species to play identical structural roles within the final crystal architecture. An isostructurality-based design would, therefore, exploit molecular assembly at the level of the entire crystal structure, rather than constructing local environments defined by individual synthons. This, however, has proven to be difficult due to the sensitivity of crystal packing to even the slightest variation in molecular structure.<sup>39–43</sup>

<sup>a</sup>Institut de Ciència de Materials de Barcelona (ICMAB-CSIC), Campus de la UAB, Bellaterra, 08193, Spain. E-mail: judit.galcera@gmail.com

<sup>b</sup>Department of Chemistry, University of Cambridge, Lensfield Road, Cambridge, CB21EW, United Kingdom. E-mail: wj10@cam.ac.uk

<sup>c</sup>School of Pharmacy, University of East Anglia, Norwich, NR4 7TJ, United Kingdom

† Electronic supplementary information (ESI) available: Details on experimental characterization by PXRD, FTIR-ATR, thermal analyses crystal structure determination from SCXRD and PXRD, and computational studies. CCDC 856200–856214. For ESI and crystallographic data in CIF or other electronic format see DOI: 10.1039/c2ce25550b

We now describe a family of organic inclusion binary-hosts where the isostructurality is sufficiently robust to allow the systematic and precise modification of the shape and size of the guest inclusion cavity. While the structural robustness of the binary-host framework allows the decoration of the inclusion pore walls with a variety of chemical functionalities as well as control over pore size, shape and chirality, it also enables the host structure to distinguish between guests exhibiting small differences in shape and size.

We have recently reported isostructurality in three salts of the pharmaceutical compound lamotrigine [3,5-diamino-6-(2,3-dichlorophenyl)-1,2,4-triazine, **LM**].<sup>44</sup> The crystal structure of these solids is based on the combination of **LM** cations and a 1,4-butanedicarboxylate anion (**DC**) to form a two-component salt inclusion binary-host (**LM+DC**), along with an included guest molecule (Fig. 1a). The combination of **LM** with fumaric, succinic and D,L-tartaric acids revealed unexpectedly robust isostructurality for these salt hosts. We recognised such preliminary evidence for robustness as an opportunity to attempt fine-tuning of the potential inclusion space in a systematic way by variation in the acid molecular structure using a set of acids modified along the carbon backbone with different substituents: acetylenedicarboxylic (**1**), fumaric (**2**), succinic (**3**), D-tartaric (**4**), L-tartaric (**5**), D-malic (**6**), L-malic (**7**), mesaconic (**8**), D,L-chlorosuccinic (**9**), D,L-bromosuccinic (**10**), 2,2-difluorosuccinic (**11**) and *meso*-2,3-dibromosuccinic (**12**) acids. Potential guests

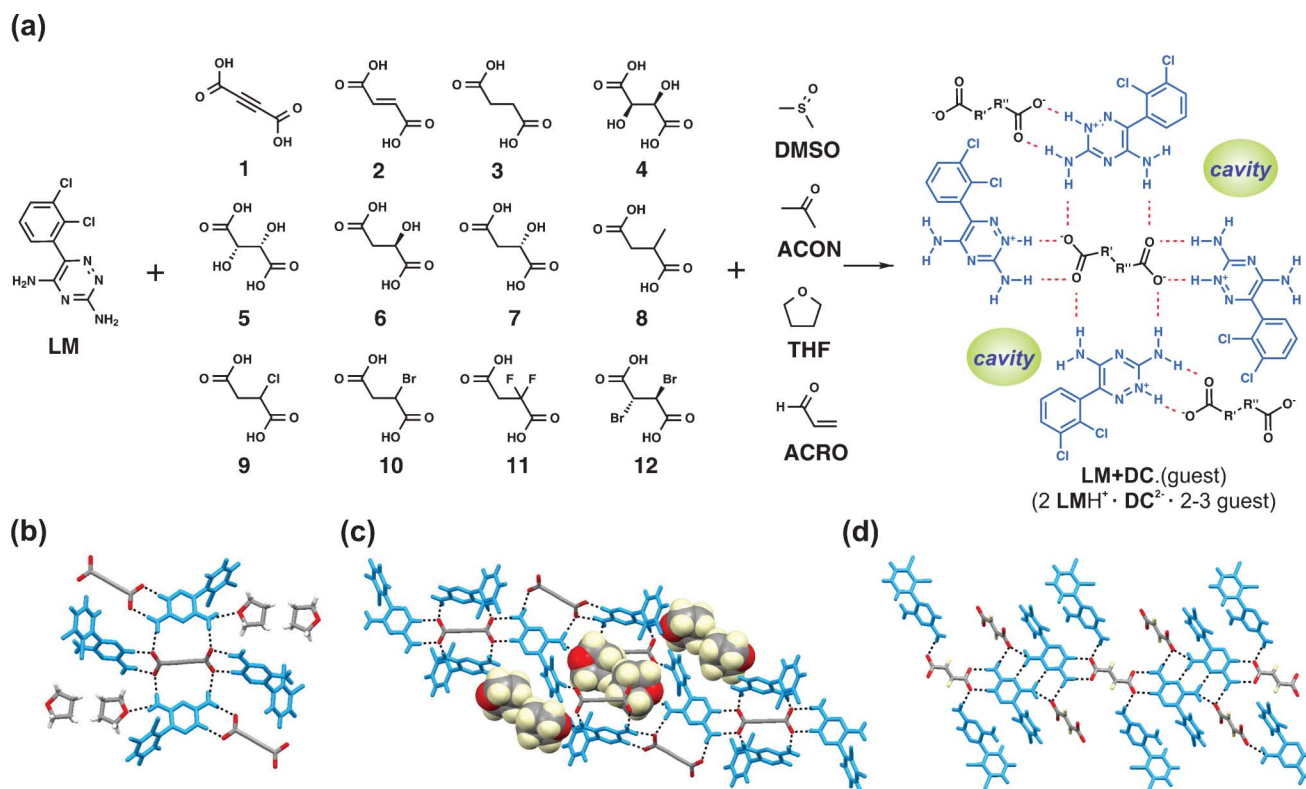
selected were dimethyl sulfoxide (DMSO), acetone (ACON), tetrahydrofuran (THF) and acrolein (ACRO) (Fig. 1a). Such a range of acids we believed would allow for controlled variation in the nature of the inclusion cavities and hence selectivity of different guests. As the synthesis of multi-component organic materials in solution is often limited by the solubilities of individual components, we have used the more efficient liquid-assisted grinding (LAG) screening technique to screen for product formation.<sup>24,45,46</sup>

## Results

### LAG screening

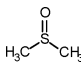
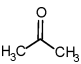

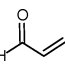
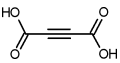
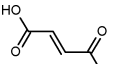
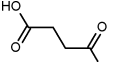
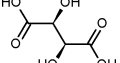
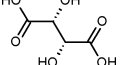
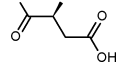
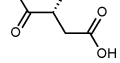
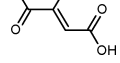
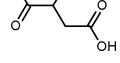
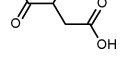
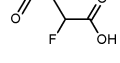
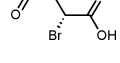
The comparison of the results of the LAG screening for reactivity between **LM** and the various acids in the presence of different guests are summarized in Table 1, along with the information on the stability of the obtained materials (as evaluated by powder X-ray diffraction (PXRD) following ageing for two weeks). Our screen revealed a set of 34 isostructural three-component solids.

The guest DMSO readily formed isostructural **LM+DC** binary-hosts with all the acids, while ACON is included in all **LM+DC** binary-hosts except **LM+11**. The larger THF and the smaller ACRO guest molecules exhibited a more selective incorporation: THF was included in six-binary hosts (**LM+1** to



**Fig. 1** Formation of isostructural host-guest adducts. (a) Combination of lamotrigine (**LM**) with the dicarboxylic acids **1** to **12** and the guests DMSO, ACON, THF and ACRO gives rise to the general structure of the **LM+DC** binary-host, where cavity indicates the location of the guest molecules; (b) crystal packing diagram of the **LM+1**·(THF) structure showing the two main hydrogen-bonded  $R_2^2(8)$  and  $R_2^2(13)$  synthons between **LM** (blue) and the acid and the hydrogen bonding interactions between **LM** and THF and (c) crystal packing of the **LM+1**·(THF) structure showing the THF guest (space-filling) in the cavities limited by the dichlorophenyl and triazine groups of the **LM** (blue) and the carbon backbone of **1**. (d) Diagram of the single crystal structure of the guest-free collapsed structure formed between **LM** and acid **2** (collapsed **LM+2**).

**Table 1** Results of the LAG experiments involving **LM** and the acids **1** to **12** with the guests DMSO, ACON, THF and ACRO. The stability of the isostructural **LM+DC**·(guest) compounds obtained by LAG was evaluated by PXRD after 15 days

		Guest solvent molecule				
		DMSO	ACON	THF	ACRO	
						
Dicarboxylic acid	<b>1</b>		✓ +	✓ +	✓ +	✓ +
	<b>2</b>		✓ +	✓ +	✓ +	✗
	<b>3</b>		✓ +	✓ -	✓ -	✗
	<b>4</b>		✓ +	✓ +	✓ +	✗
	<b>5</b>		✓ +	✓ +	✓ +	✗
	<b>6</b>		✓ +	✓ +	✗	✗
	<b>7</b>		✓ +	✓ -	✗	✗
	<b>8</b>		✓ +	✓ +	✓ +	✓ +
	<b>9</b>		✓ +	✓ +	✗	✓ +
	<b>10</b>		✓ +	✓ +	✗	✓ -
	<b>11</b>		✓ -	✗	✗	✗
	<b>12</b>		✓ +	✓ +	✗	✓ +

✓ isostructural **LM+DC**·(guest), + stable after >15 days, ✗ non-isostructural, - non-stable after >15 days.

**LM+5**, and **LM+8**) and ACRO in five (**LM+1**, **LM+8** to **LM+10**, and **LM+12**). The incorporation of THF and ACRO is almost complementary, with the only overlaps being for **LM+1** and **LM+8**. These two host systems are also the most versatile in this study, as they form host-guest complexes with all the explored guests.

## Crystal structure determination

Single crystals suitable for structure analysis were obtained for **LM+1**·(THF), **LM+2**·(DMSO), **LM+3**·(DMSO), **LM+3**·(ACON), **LM+4**·(DMSO), **LM+4**·(ACON), **LM+5**·(DMSO), **LM+6**·(DMSO), **LM+8**·(ACON), **LM+9**·(DMSO) and **LM+10**·(ACON), as well as for the mixed guest system **LM+1**·(DMSO-THF) and the guest-free collapsed salts **LM+2** and **LM+3**. While we were unable to obtain diffraction-quality single crystals of the **LM+12**·(ACON), structural characterisation was accomplished directly using PXRD data collected at the Diamond Synchrotron beamline I11.

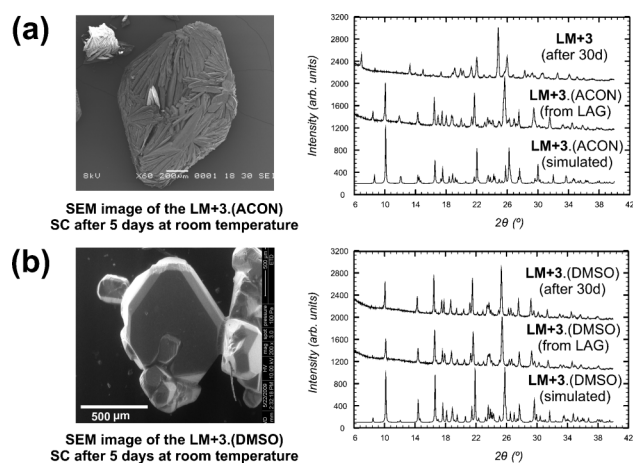
In agreement with the results of the PXRD analyses of the LAG synthesized materials (S1–S4, ESI†), all the inclusion complexes are isostructural, exhibiting almost identical crystal packing and hydrogen-bonding motifs. Each structure consists of protonated **LM** cations hydrogen-bonded to acid dianions and the guest molecules in a 2:1:2 ratio, respectively. The overall crystal architecture in each case is identical to that previously reported for **LM+DL-tartaric acid** with DMSO as the guest. Specifically, **LM** and the acid form an open hydrogen-bonded structure into which the guest is accommodated (Fig. 1b–1c and S5–S18, ESI†). The binary-host structure is sustained principally by  $R_2^2(8)$  and  $R_2^2(13)$  charge-assisted hydrogen-bonded hetero-synthons.<sup>47</sup> As each **DC** anion is connected through two  $R_2^2(13)$  synthons to two **LM** cations, the size matching of the **DC** backbone length with the distance between the two primary amine groups of **LM** is essential to achieve the isostructural binary-host architecture. The ionized nature of the **LM** and the acids is evident from the structure of the acid carboxylate group, which exhibits two similar C–O bond lengths of 1.25–1.28 Å. The formation of an ionic host in all LAG synthesised **LM+DC**·(guest) systems is also confirmed by their FTIR-ATR spectra (S19–S22, ESI†).

Within the host structure, one N–H group of each **LM** cation remains available for hydrogen bonding. These groups serve as guest docking sites through N–H···O hydrogen bonding to the guest oxygen atom. In all the structures so far determined, the host-guest hydrogen-bonding distances are in the range 2.8–2.9 Å, comparable to previously reported structures, and indicative of being of intermediate hydrogen bond strength. The guest molecules occupy cavities whose surfaces are delineated by the dichlorophenyl and aminotriazine rings of **LM** and, importantly, by the chemical functionality on the central backbone of the acid (Fig. 1c).

The structures of the guest-free collapsed salts **LM+2** and **LM+3**, which are themselves isostructural, reveal a rearrangement of the **LM** and **DC** molecules upon guest removal to form a close-packed structure. The  $R_2^2(8)$  charge-assisted hydrogen-bonded synthons between the acid and **LM** persist, but the  $R_2^2(13)$  synthon is no longer present. Instead, pairs of **LM** molecules are hydrogen-bonded to form dimeric  $R_2^2(8)$  homosynthons (Fig. 1d and S16, ESI†). The remaining N–H groups of the **LM** form dimers by bifurcated hydrogen bonds to a neighbouring carboxylate group.

## Stability and reversible dynamic inclusion

Chemical modification of the dicarboxylic acid introduces significant changes to the guest binding properties of the **LM+DC** binary-hosts.<sup>48</sup> In the majority of cases, heating of the complex results in guest loss and framework collapse to form



**Fig. 2** Variable stability of **LM+DC**·(guest) compounds. SEM images show spontaneous recrystallization to collapsed **LM+3** from single crystals (SC) of **LM+3**·(ACON) (a) and stable behaviour for **LM+3**·(DMSO) crystals (b). Comparison of PXRD patterns of the LAG synthesized **LM+3**·(ACON) and **LM+3**·(DMSO) before and after 30 days ageing at ambient conditions with corresponding simulated patterns also indicates no change for **LM+3**·(DMSO) and complete decomposition of **LM+3**·(ACON) to form collapsed **LM+3**.

**LM+DC** salts (Fig. 2). The temperature of decomposition was observed to be in the range 90–140 °C for the ACON systems (S23, ESI†), the precise value varying with the choice of acid: **LM+3**·(ACON), for example decomposed at room temperature to form the collapsed **LM+3** salt, while **LM+1**·(ACON) and **LM+5**·(ACON) do not release ACON until complete thermal decomposition above 140 °C. The collapsed **LM+3** salt is crystalline, as characterised by scanning electron microscopy and PXRD (Fig. 2). The formation of a crystalline collapsed **LM+DC** salt was also observed following decomposition of **LM+3**·(THF), **LM+7**·(ACON) and **LM+11**·(DMSO) after two weeks of ageing (Table 1).

The exposure of the collapsed **LM+DC** salts to ACON vapours for 20 h revealed reversibility of the inclusion, dependent on the identity of the acid (Fig. S25, ESI†). The formation of binary-hosts **LM+2**, **LM+4**, **LM+8** and **LM+9**, leading to ACON inclusion compounds was fully reversible as verified by PXRD and TG analyses. Such reversibility led us to

test the formation of the **LM+DC** binary-hosts by exposing the physical mixtures of crystalline **LM** and **DC** to ACON vapours. Indeed, the complete formation of **LM+DC**·(ACON) was observed after 20 h for **LM+1**, **LM+2**, **LM+4**, **LM+6**, **LM+8**, **LM+9**, **LM+10** and **LM+12**.

### Computational studies

In order to understand the robustness of the **LM+DC** isostructural binary-host framework, lattice energies were calculated and compared for **LM+1**, **LM+2** and **LM+3** containing DMSO, ACON and THF as guests (Table 2). Considering the experimentally determined X-ray structures of the **LM+DC**·(DMSO) compounds, two guest molecules were assumed to occupy the cavity in each modelled structure. Lattice energies were also calculated for the collapsed salts **LM+2** and **LM+3** experimentally obtained after guest loss, and for the hypothetical empty frameworks **LM+1**, **LM+2** and **LM+3** obtained by removing the coordinates of the guests from the experimentally determined X-ray structures **LM+1**·(DMSO), **LM+2**·(DMSO) and **LM+3**·(DMSO). Because of the industrial importance of ACRO, we also modelled its inclusion for all the **LM+DC** binary-hosts, again assuming two molecules per cavity.

In all cases, lattice energy minimization of the hypothetical empty frameworks resulted in only very small changes in lattice parameters (Table S26, ESI†). The arrangement of **LM** and the acid was virtually unchanged, indicating that the hypothetical empty frameworks are robust local minima on the **LM+DC** lattice energy surfaces. Comparison with the calculated lattice energies of the collapsed **LM+DC** structures, however, suggested that the hypothetical empty frameworks are much less stable than the corresponding collapsed structures experimentally obtained after guest loss: *e.g.* collapsed **LM+2** is found to be 31.5 kJ mol<sup>-1</sup> more stable than the hypothetical empty **LM+2**, and the collapsed **LM+3** is 29.3 kJ mol<sup>-1</sup> more stable than the hypothetical empty **LM+3**. Structures with included guests would only be favoured over the collapsed alternatives if the guest formed interactions with the framework which overcome the ~30 kJ mol<sup>-1</sup> lattice energy difference, as well as the enthalpic and entropic cost of removing the guests from the liquid phase.

Calculated lattice energies of all isostructural guest-containing salts are similar in magnitude (Table 2) and comparison with the empty frameworks yields the stabilisation energy provided by

**Table 2** Lattice energies [ $E_{\text{latt}}$  (kJ mol<sup>-1</sup>)], packing coefficients ( $C_{\text{pack}}$ ) and solvent accessible volumes [ $V_{\text{SA}}$  (Å<sup>3</sup>)] in the energy minimized solvated **LM+DC**·(guest) and hypothetical desolvated crystal structures (**LM+1**, **LM+2**). Energies are given per mol of the formula unit (2 **LM** + 1 **DC** + included solvent). Solvent accessible volumes were calculated using a probe of radius 1.2 Å and a grid step of 0.2 Å

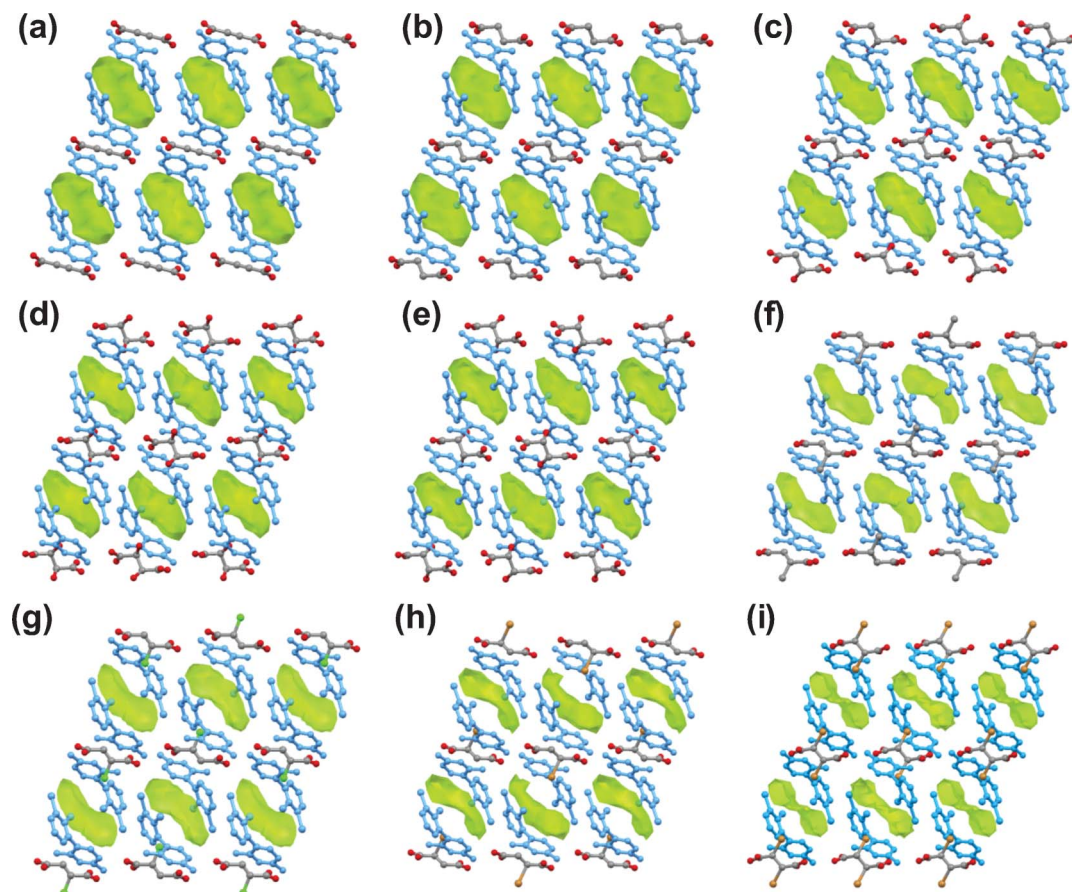
		<b>LM+DC</b> ·(guest)				<b>LM+DC</b> hypothetical framework
		DMSO	ACON	THF	ACRO	
<b>LM+1</b>	$E_{\text{latt}}$	-860.6	-840.5	-837.1	-834.3	-754.1
	$C_{\text{pack}}$	0.67	0.64	0.66	0.61	0.50
	$V_{\text{SA}}$	0	0	10	33	273
<b>LM+2</b>	$E_{\text{latt}}$	-863.5	-845.6	-841.2	-838.2	-758.0
	$C_{\text{pack}}$	0.67	0.66	0.67	0.67	0.52
	$V_{\text{SA}}$	0	10	8	0	268
<b>LM+3</b>	$E_{\text{latt}}$	-872.5	-846.7	-845.7	-839.4	-759.2
	$C_{\text{pack}}$	0.67	0.63	0.65	0.65	0.46
	$V_{\text{SA}}$	0	22	0	0	299

incorporation of guests into the cavity (Table S27, ESI†). The values range from 80 to 113 kJ mol<sup>-1</sup> (for inclusion of two guest molecules). For a given guest, variations between **LM+1**, **LM+2** and **LM+3** introduce small variations in the stabilisation energy and only slightly influences the size and shape of the cavity (Fig. 3). However, crystal structure stabilisation follows a clear trend amongst the guests with stabilisation decreasing across the series: DMSO > ACON > THF > ACRO. For all systems, the lattice energy gained is close to or slightly greater than the enthalpy required to remove two molecules from the liquid phase [ $\Delta H_{\text{vap}}^{\circ}(\text{DMSO}) \approx 53$  kJ mol<sup>-1</sup>,  $\Delta H_{\text{vap}}^{\circ}(\text{ACON}) \approx 31$  kJ mol<sup>-1</sup>,  $\Delta H_{\text{vap}}^{\circ}(\text{THF}) \approx 32$  kJ mol<sup>-1</sup> and  $\Delta H_{\text{vap}}^{\circ}(\text{ACRO}) \approx 28$  kJ mol<sup>-1</sup>].

## Discussion

That structural robustness of the **LM+DC** framework allows the modification of the size and shape of the inclusion cavity is clearly demonstrated by the comparison of **LM+1**·(THF), **LM+3**·(DMSO), **LM+9**·(DMSO) and **LM+10**·(ACON) structures. These structures reveal that the cavity shape, as well as volume, can be tailored by changing the functional groups on the carbon backbone of the acid (Fig. 3). Increasing the size of the functional group for a monosubstituted acid distorts the oval (in

**LM+1**·(THF) inclusion cavity in a non-symmetrical fashion (e.g. in **LM+9**·(THF)). For vicinally disubstituted acids, the increase in substituent size leads to compartmentalisation of the inclusion cavity and the formation of a symmetrical “bottleneck” (as seen in **LM+4**·(guest)). In the case of the large bromine atom substituent, the result is almost a splitting of the inclusion cavity (**LM+12**·(ACON), Fig. 3i). In addition to modification to the overall shape and topology of the inclusion pore, variation of the substituent on the acids **1–12** results in a pore decoration with alkyne groups, fluorocarbon and saturated and unsaturated hydrocarbon moieties, symmetrically- and asymmetrically-disposed hydroxyl moieties, as well as halogen atoms of variable size (Cl and Br). In this process, the volume of the voids<sup>43</sup> varied between 286 Å<sup>3</sup> (**LM+1**) and 230 Å<sup>3</sup> (**LM+8**). As evidenced by the LAG experiments, this leads to selective inclusion in the isostructural binary-hosts. The similarity in inclusion behaviour of DMSO and ACON, which are included in almost all the explored binary-hosts, is not surprising as the molecules are comparable in size and polarity. However, the inclusion of THF and ACRO follows opposite trends, related to the relative sizes of guests and inclusion pores. The larger THF is included in binary-hosts **LM+1** through to **LM+8**, with inclusion pores of 286–230 Å<sup>3</sup> volume, while the smaller ACRO is included in



**Fig. 3** Modulation of the morphology and size of the inclusion cavities in selected **LM+DC** binary-hosts. Inclusion cavities in the single crystal structures of: (a) **LM+1**·(THF); (b) **LM+3**·(DMSO); (c) **LM+6**·(DMSO); (d) **LM+4**·(DMSO); (e) **LM+5**·(DMSO); (f) **LM+8**·(DMSO); (g) **LM+9**·(DMSO); (h) **LM+10**·(ACON) and (i) **LM+12**·(ACON) with guest molecules removed for clarity. The representations of the cavity voids (green) accessible to spherical guest molecules of 1.4 Å radius show the **DC**-dependent progressive modification of the cavities. The **LM** molecules are drawn in blue and the hydrogen atoms were removed for clarity.

**Table 3** Crystal data and structure refinement data for **LM+1**·(DMSO-THF), **LM+1**·(THF), **LM+2**·(DMSO) and the guest-free salts **LM+2** and **LM+3**

Compound reference	<b>LM+1</b> ·(DMSO-THF)	<b>LM+1</b> ·(THF)	<b>LM+2</b>	<b>LM+2</b> ·(DMSO)	<b>LM+3</b>
Chemical formula	2(C <sub>9</sub> H <sub>8</sub> Cl <sub>2</sub> N <sub>5</sub> ) C <sub>4</sub> O <sub>4</sub> 1.6(C <sub>4</sub> H <sub>8</sub> O) 0.4(C <sub>2</sub> H <sub>6</sub> OS)	2(C <sub>9</sub> H <sub>8</sub> Cl <sub>2</sub> N <sub>5</sub> ) C <sub>4</sub> O <sub>4</sub> 2(C <sub>4</sub> H <sub>8</sub> O)	2(C <sub>9</sub> H <sub>8</sub> Cl <sub>2</sub> N <sub>5</sub> ) C <sub>4</sub> H <sub>2</sub> O <sub>4</sub>	2(C <sub>9</sub> H <sub>8</sub> Cl <sub>2</sub> N <sub>5</sub> ) C <sub>4</sub> H <sub>2</sub> O <sub>4</sub> 2(C <sub>2</sub> H <sub>6</sub> OS)	2(C <sub>9</sub> H <sub>8</sub> Cl <sub>2</sub> N <sub>5</sub> ) C <sub>4</sub> H <sub>4</sub> O <sub>4</sub>
Formula Mass	772.87	770.45	628.26	784.52	630.28
Crystal system	Monoclinic	Monoclinic	Monoclinic	Monoclinic	Monoclinic
<i>a</i> /Å	11.0783(2)	11.2006(3)	12.8481(3)	10.6601(2)	12.8921(4)
<i>b</i> /Å	10.3174(2)	10.2189(2)	9.1579(2)	10.9576(2)	9.2100(2)
<i>c</i> /Å	16.3132(3)	16.3395(5)	11.2303(3)	15.8831(3)	11.1833(3)
<i>α</i> /°	90.00	90.00	90.00	90.00	90.00
<i>β</i> /°	108.6390(10)	109.0430(10)	100.928(2)	108.7680(10)	101.290(10)
<i>γ</i> /°	90.00	90.00	90.00	90.00	90.00
Unit cell volume/Å <sup>3</sup>	1766.79(6)	1767.84(8)	1297.41(5)	1756.64(6)	1302.17(6)
Temperature/K	180(2)	180(2)	180(2)	180(2)	180(2)
Space group	<i>P</i> 2 <sub>1</sub> / <i>c</i>	<i>P</i> 2 <sub>1</sub> / <i>c</i>	<i>P</i> 2 <sub>1</sub> / <i>c</i>	<i>P</i> 2 <sub>1</sub> / <i>n</i>	<i>P</i> 2 <sub>1</sub> / <i>c</i>
No. of formula units per unit cell, <i>Z</i>	2	2	2	2	2
Absorption coefficient, μ/mm <sup>-1</sup>	0.416	0.392	0.509	0.511	0.507
No. of reflections measured	21 444	12 205	13 165	29 063	11 994
No. of independent reflections	5573	5115	1353	6992	2289
<i>R</i> <sub>int</sub>	0.0360	0.0330	0.0347	0.0300	0.0392
Final <i>R</i> <sub>1</sub> values ( <i>I</i> > 2σ( <i>I</i> ))	0.0469	0.0463	0.0415	0.0535	0.0448
Final <i>wR</i> ( <i>F</i> <sup>2</sup> ) values ( <i>I</i> > 2σ( <i>I</i> ))	0.1155	0.1048	0.0876	0.1480	0.1141
Final <i>R</i> <sub>1</sub> values (all data)	0.0753	0.0633	0.0430	0.0678	0.0554
Final <i>wR</i> ( <i>F</i> <sup>2</sup> ) values (all data)	0.1375	0.1155	0.0882	0.1607	0.1305
Goodness of fit on <i>F</i> <sup>2</sup>	1.056	1.049	1.203	1.060	1.196
Largest diff. peak and hole/e Å <sup>-3</sup>	0.638 and -0.472	0.360 and -0.386	0.216 and -0.196	0.759 and -0.855	0.203 and -0.315
Wavelength/Å	0.71070	0.71070	0.71070	0.71070	0.71070
CCDC number	856200	856201	856202	856203	856204

**LM+1**, as well as in **LM+8**, **LM+9** and **LM+10**. The binary-hosts **LM+8**, **LM+9** and **LM+10** have pore sizes of 230–263 Å<sup>3</sup>. With the exception of the **LM+1**·(ACRO), such selectivity in inclusion is consistent with close packing of molecules, with ACRO being too small to fill the cavities of binary-hosts **LM+2** to **LM+8**, and THF too large to fit into pores of **LM+8** to **LM+10**. The exceptional formation of **LM+1**·(ACRO) can be rationalised by the inclusion of more than two molecules of

ACRO within the significantly large cavity of the **LM+1** binary-host. This is supported by thermogravimetric analysis, which indicated the loss of three equivalents of ACRO per cavity. Void space calculations using a 1.2 Å radius probe on the energy-minimized **LM+DC**·(guest) systems (Table 2) demonstrate that the two guest molecules fill the cavity efficiently in all but a few systems studied; there is no residual accessible volume in seven of the twelve modelled structures and only 8–10 Å<sup>3</sup> of guest-accessible volume in

**Table 4** Crystal data and structure refinement data for **LM+3**·(ACON), **LM+3**·(DMSO), **LM+4**·(ACON), **LM+4**·(DMSO) and **LM+5**·(DMSO)

Compound reference	<b>LM+3</b> ·(ACON)	<b>LM+3</b> ·(DMSO)	<b>LM+4</b> ·(ACON)	<b>LM+4</b> ·(DMSO)	<b>LM+5</b> ·(DMSO)
Chemical formula	2(C <sub>9</sub> H <sub>8</sub> Cl <sub>2</sub> N <sub>5</sub> ) C <sub>4</sub> H <sub>4</sub> O <sub>4</sub> 2(C <sub>3</sub> H <sub>6</sub> O)	2(C <sub>9</sub> H <sub>8</sub> Cl <sub>2</sub> N <sub>5</sub> ) C <sub>4</sub> H <sub>4</sub> O <sub>4</sub> 2(C <sub>2</sub> H <sub>6</sub> OS)	2(C <sub>9</sub> H <sub>8</sub> Cl <sub>2</sub> N <sub>5</sub> ) C <sub>4</sub> H <sub>4</sub> O <sub>6</sub> 2(C <sub>3</sub> H <sub>6</sub> O)	2(C <sub>9</sub> H <sub>8</sub> Cl <sub>2</sub> N <sub>5</sub> ) C <sub>4</sub> H <sub>4</sub> O <sub>6</sub> 2(C <sub>2</sub> H <sub>6</sub> OS)	2(C <sub>9</sub> H <sub>8</sub> Cl <sub>2</sub> N <sub>5</sub> ) C <sub>4</sub> H <sub>4</sub> O <sub>6</sub> 2(C <sub>2</sub> H <sub>6</sub> OS)
Formula Mass	746.43	786.54	778.44	818.54	818.54
Crystal system	Monoclinic	Monoclinic	Monoclinic	Monoclinic	Monoclinic
<i>a</i> /Å	10.8143(3)	11.0200(2)	10.7524(2)	11.09580(10)	11.09610(10)
<i>b</i> /Å	10.7320(3)	10.6723(2)	11.3284(2)	11.0374(2)	11.04200(10)
<i>c</i> /Å	16.0105(4)	15.9451(3)	15.5321(3)	15.6848(2)	15.6858(2)
<i>α</i> /°	90.00	90.00	90.00	90.00	90.00
<i>β</i> /°	108.5600(10)	108.8400(10)	105.0240(10)	106.9470(10)	106.9500(10)
<i>γ</i> /°	90.00	90.00	90.00	90.00	90.00
Unit cell volume/Å <sup>3</sup>	1761.52(8)	1774.81(6)	1827.25(6)	1837.48(4)	1838.39(3)
Temperature/K	180(2)	180(2)	180(2)	180(2)	180(2)
Space group	<i>P</i> 2 <sub>1</sub> / <i>c</i>	<i>P</i> 2 <sub>1</sub> / <i>c</i>	<i>P</i> 2 <sub>1</sub>	<i>P</i> 2 <sub>1</sub>	<i>P</i> 2 <sub>1</sub>
No. of formula units per unit cell, <i>Z</i>	2	2	2	2	2
Absorption coefficient, μ/mm <sup>-1</sup>	0.391	0.506	0.384	0.495	0.495
No. of reflections measured	13658	18322	21966	21241	41755
No. of independent reflections	6590	6129	9677	11316	13499
<i>R</i> <sub>int</sub>	0.0308	0.0352	0.0262	0.0283	0.0242
Final <i>R</i> <sub>1</sub> values ( <i>I</i> > 2σ( <i>I</i> ))	0.0520	0.0425	0.0457	0.0367	0.0358
Final <i>wR</i> ( <i>F</i> <sup>2</sup> ) values ( <i>I</i> > 2σ( <i>I</i> ))	0.1117	0.1081	0.1126	0.0913	0.0923
Final <i>R</i> <sub>1</sub> values (all data)	0.0770	0.0561	0.0629	0.0417	0.0413
Final <i>wR</i> ( <i>F</i> <sup>2</sup> ) values (all data)	0.1262	0.1189	0.1268	0.0955	0.0969
Goodness of fit on <i>F</i> <sup>2</sup>	1.067	1.063	1.092	1.046	1.034
Largest diff. peak and hole/e Å <sup>-3</sup>	0.353 and -0.430	0.502 and -0.470	0.510 and -0.317	0.357 and -0.402	0.650 and -0.435
Wavelength/Å	0.71070	0.71070	0.71070	0.71070	0.71070
CCDC number	856206	856205	856208	856207	856209

**Table 5** Crystal data and structure refinement data for **LM+6**·(DMSO), **LM+8**·(ACON), **LM+9**·(DMSO), **LM+10**·(ACON) and **LM+12**·(ACON)

Compound reference	<b>LM+6</b> ·(DMSO)	<b>LM+8</b> ·(ACON)	<b>LM+9</b> ·(DMSO)	<b>LM+10</b> ·(ACON)	<b>LM+12</b> ·(ACON)
Chemical formula	2(C <sub>9</sub> H <sub>8</sub> Cl <sub>2</sub> N <sub>5</sub> ) C <sub>4</sub> H <sub>4</sub> O <sub>5</sub> 2(C <sub>2</sub> H <sub>6</sub> OS)	2(C <sub>9</sub> H <sub>8</sub> Cl <sub>2</sub> N <sub>5</sub> ) C <sub>3</sub> H <sub>4</sub> O <sub>4</sub> C <sub>4</sub> H <sub>9</sub> NO <sub>3</sub>	2(C <sub>9</sub> H <sub>8</sub> Cl <sub>2</sub> N <sub>5</sub> ) 2(C <sub>2</sub> H <sub>6</sub> OS) C <sub>4</sub> H <sub>3</sub> ClO <sub>4</sub>	2(C <sub>9</sub> H <sub>8</sub> Cl <sub>2</sub> N <sub>5</sub> ) C <sub>4</sub> H <sub>3</sub> BrO <sub>4</sub> 2(C <sub>3</sub> H <sub>6</sub> O)	2(C <sub>9</sub> H <sub>8</sub> Cl <sub>2</sub> N <sub>5</sub> ) C <sub>4</sub> H <sub>2</sub> Br <sub>2</sub> O <sub>4</sub> 2(C <sub>3</sub> H <sub>6</sub> O)
Formula Mass	802.54	761.41	820.98	825.34	904.22
Crystal system	Monoclinic	Monoclinic	Monoclinic	Monoclinic	Monoclinic
<i>a</i> /Å	11.0150(2)	10.6172(2)	11.0489(3)	10.7609(3)	11.26187(16)
<i>b</i> /Å	10.8376(2)	10.9788(2)	10.8220(4)	11.0390(4)	11.19534(9)
<i>c</i> /Å	15.9178(3)	15.9940(4)	16.2310(7)	16.0899(6)	16.38551(25)
<i>α</i> /°	90.00	90.00	90.00	90.00	90.0
<i>β</i> /°	108.1110(10)	109.1290(10)	109.403(2)	107.284(2)	110.8611(9)
<i>γ</i> /°	90.00	90.00	90.00	90.00	90.0
Unit cell volume/Å <sup>3</sup>	1806.06(6)	1761.38(6)	1830.53(12)	1825.00(11)	1930.47(4)
Temperature/K	180(2)	180(2)	180(2)	180(2)	293
Space group	<i>P</i> 2 <sub>1</sub>	<i>P</i> 2 <sub>1</sub> / <i>c</i>	<i>P</i> 2 <sub>1</sub> / <i>c</i>	<i>P</i> 2 <sub>1</sub> / <i>c</i>	<i>P</i> 2 <sub>1</sub> / <i>c</i>
No. of formula units per unit cell, <i>Z</i>	2	2	2	2	2
Absorption coefficient, μ/mm <sup>-1</sup>	0.500	0.392	0.564	1.473	
No. of reflections measured	22 975	11 790	12 846	10 039	1685
No. of independent reflections	8323	4653	4173	4110	
<i>R</i> <sub>int</sub>	0.0411	0.0273	0.0410	0.0301	
Final <i>R</i> <sub>1</sub> values ( <i>I</i> > 2σ( <i>I</i> ))	0.0468	0.0562	0.0939	0.0798	
Final <i>wR</i> ( <i>F</i> <sup>2</sup> ) values ( <i>I</i> > 2σ( <i>I</i> ))	0.1125	0.1370	0.2467	0.1996	
Final <i>R</i> <sub>1</sub> values (all data)	0.0713	0.0656	0.1300	0.0993	
Final <i>wR</i> ( <i>F</i> <sup>2</sup> ) values (all data)	0.1333	0.1445	0.2731	0.2136	
Final <i>R</i> <sub>wp</sub>					0.0365
Final <i>R</i> <sub>p</sub>					0.0363
Goodness of fit on <i>F</i> <sup>2</sup>	1.100	1.044	1.155	1.055	1.98
Largest diff. peak and hole/e Å <sup>-3</sup>	0.633 and -0.329	0.729 and -0.590	0.635 and -0.469	1.008 and -0.780	0.44 and -0.42
Wavelength/Å	0.71070	0.71070	0.71070	0.71070	1.06237
CCDC number	856210	856211	856212	856213	856214

a further three structures (**LM+2**·(ACON), **LM+1**·(THF) and **LM+2**·(THF)). Only two of the modelled solvated structures contain significant residual accessible volume with two guests located in the cavity: **LM+1**·(ACRO) (33 Å<sup>3</sup>) and **LM+3**·(ACON) (22 Å<sup>3</sup>). We estimate the molecular volume of ACRO to be approximately 60 Å<sup>3</sup> and, by rearrangement of the first two guest molecules in **LM+1**·(ACRO), it seems possible to sufficiently increase the accessible volume to host a third guest. Three ACRO molecules would fill the 273 Å<sup>3</sup> cavity in the energy-minimized **LM+1** with 65% efficiency, a typical packing coefficient for molecular crystals. For **LM+3**·(ACON), two guest molecules clearly do not adequately fill the cavity. However, in this case there is less guest-accessible volume in the cavity and a third molecule cannot be accommodated. The low stability of **LM+3**·(ACON) (Table 1) could be related to the poor efficiency with which the two guest molecules fill the cavity.

## Conclusions

In conclusion, we have discovered a remarkable family of inclusion binary-hosts based on a two-component ionic structure which is sufficiently robust to allow modifications to the shape and the surface functionalities of the inclusion cavity. In addition to the growth from solution, the inclusion hosts can be assembled by exposing a mixture of solid components to a suitable guest in the liquid or gas state, with or without mechanical agitation. While the binary-host structure is not stable upon guest loss, our study reveals that variation in the components of the binary-host can also be used to determine the reversibility or not of the host-guest assembly process. We expect that further studies of molecular host assembly through liquid-solid and gas-solid reactions will provide new opportunities for permanent binding or the reversible

inclusion of guests, while understanding of robust isostructurality reported herein could provide the self-assembled molecular systems with the same level of versatility as established for metal-organic materials.

## Methods

### Liquid-assisted grinding (LAG)

LAG experiments were performed by placing 100 mg of physical mixture of crystalline powders of **LM** with the corresponding **DC** (**1** to **12**) in a 2:1 stoichiometric ratio into a 10 mL stainless-steel grinding jar, this accompanied by the addition of 50 to 70 μL of the potential guest solvent molecules (DMSO, ACON, THF, ACRO). Grinding experiments were performed using a Retsch MM200 grinding mill over a period of 20 min, at a rate of 30 Hz, using two stainless-steel grinding balls (7 mm diameter). The obtained products were characterized by powder X-ray diffraction (PXRD), Fourier-transform infrared attenuated total reflectance spectroscopy (FTIR-ATR) and thermal analyses (DSC and TGA). Further details on PXRD, FTIR-ATR and thermal analyses are given in the ESI.†

### Single crystal growth

Crystals used for single crystal X-ray diffraction analyses were obtained by slow evaporation of solutions prepared by dissolving the previously LAG synthesized materials in the appropriate solvents or solvent mixtures.

### Reversible guest inclusion experiments

The **LM+DC**·(ACON) compounds prepared by LAG were dried for 20 h in a vacuum oven at 100 °C to obtain the collapsed



**LM+DC** salts. After being analysed these samples were exposed to ACON vapours for 20 h and subsequently analysed.

### Powder X-ray diffraction (PXRD)

PXRD data used for crystal structure solution of **LM+12**·(ACON) was collected at the Diamond Synchrotron beamline I11 using a radiation wavelength of 1.06237 Å and at a temperature of 293 K. Further details on crystal structure solution and refinement are given in the ESI† and Table 5.

### Single-crystal X-ray diffraction (SCXRD)

Data was collected at 180(2) K with a Nonius Kappa CCD diffractometer using MoK<sub>α</sub> radiation ( $\lambda = 0.71073$  Å) at 40 kV and 40 mA and equipped with an Oxford Cryosystems cryostream. Further details on SCXRD analyses are given in the ESI† and Tables 3–5.

### Computational methods

Lamotrigine and acid molecular structures were taken from the experimentally determined **LM+DC**·(guest) crystal structures; heavy atom positions were kept as determined in the crystal structures, while hydrogen atom positions were optimised at the B3LYP/6-31G(d,p) level of theory within Gaussian03.<sup>49</sup> All guest molecule geometries were fully optimised, also using B3LYP/6-31G(d,p). Crystal structure calculations were performed using the DMAREL lattice energy minimisation software, which is now maintained as DMACRYS.<sup>50</sup> Further details on computational methods are given in the ESI.†

### Acknowledgements

We thank Consejo Superior de Investigaciones Científicas and the European Social Fund for a PhD grant (JG) and the Pfizer Institute for Pharmaceutical Materials Science (KEH). Herchel Smith fund is acknowledged for a Research Fellowship (TF) and so is the Royal Society (GMD). Dr John E. Davies is acknowledged for single crystal X-ray diffraction data collection. Dr Andrew Cassidy is acknowledged for his help with the collection of SEM images. The Generalitat de Catalunya (Project SGR2009-203) and the Spanish Ministerio de Economía y Competitividad (Projects CSD2007-00041 and CTQ2009-12520-C03-03) are acknowledged for financial support of this research. We thank the EU INTERREG IVA 2 Mers-Seas-Zeeën Programme for financial support. Diamond Light Source (DLS, Didcot UK) is acknowledged for support, and in particular the DLS staff and scientists Chiu Tang and Julia E. Parker for beam time and technical support. The authors acknowledge Mr Dinesh-Ramesh Mirpuri Vatvani for his help with preparing the cover artwork image.

### References

- 1 G. R. Desiraju *Crystal engineering. The design of organic solids*. Elsevier, Amsterdam, 1989.
- 2 B. Moulton and M. J. Zaworotko, *Chem. Rev.*, 2001, **101**, 1629.
- 3 G. R. Desiraju, *Angew. Chem., Int. Ed. Engl.*, 1995, **34**, 2311.
- 4 G. R. Desiraju, *Nature*, 2001, **412**, 397.
- 5 C. Janiak, *Dalton Trans.*, 2003, 2781.
- 6 S. Kitagawa, R. Kitaura and S. Noro, *Angew. Chem., Int. Ed.*, 2004, **43**, 2334.

- 7 U. Mueller, M. Schubert, F. Teich, H. Puetter, K. Schierle-Arndt and J. Pastré, *J. Mater. Chem.*, 2006, **16**, 626.
- 8 P. Horcajada, T. Chalati, C. Serre, B. Gillet, C. Sebrie, T. Baati, J. F. Eubank, D. Heurtaux, P. Clayette, C. Kreuz, J. S. Chang, Y. K. Hwang, V. Marsaud, P. N. Bories, L. Cynober, S. Gil, G. Férey, P. Couvreur and R. Gref, *Nat. Mater.*, 2009, **9**, 172.
- 9 M. Eddaoudi, D. B. Moler, H. Li, B. Chen, T. M. Reineke, M. O'Keeffe and O. M. Yaghi, *Acc. Chem. Res.*, 2001, **34**, 319.
- 10 H. Li, M. Eddaoudi, M. O'Keeffe and O. M. Yaghi, *Nature*, 1999, **402**, 276.
- 11 J. S. Seo, D. Whang, H. Lee, S. I. Jun, J. Oh, Y. J. Jeon and K. Kim, *Nature*, 2000, **404**, 982.
- 12 G. R. Desiraju, *Acc. Chem. Res.*, 2002, **35**, 565.
- 13 P. Metrangolo and G. Resnati, *Chem.–Eur. J.*, 2001, **7**, 2511.
- 14 M. C. Etter, *Acc. Chem. Res.*, 1990, **23**, 120.
- 15 S. G. Fleischman, S. S. Kuduva, J. A. McMahon, B. Moulton, R. D. B. Walsh, N. Rodríguez-Hornedo and M. J. Zaworotko, *Cryst. Growth Des.*, 2003, **3**, 909.
- 16 S. L. Childs, L. J. Chyall, J. T. Dunlap, V. N. Smolenskaya, B. C. Stahly and G. P. Stahly, *J. Am. Chem. Soc.*, 2004, **126**, 13335.
- 17 A. V. Trask, W. D. S. Motherwell and W. Jones, *Cryst. Growth Des.*, 2005, **5**, 1013.
- 18 S. Karki, T. Friščić, L. Fábián, P. R. Laity, G. M. Day and W. Jones, *Adv. Mater.*, 2009, **21**, 3905.
- 19 K. Sada, N. Shiomi and M. Miyata, *J. Am. Chem. Soc.*, 1998, **120**, 10543.
- 20 K. Sada, K. Inoue, T. Tanaka, A. Tanaka, A. Epergyes, S. Nagahama, A. Matsumoto and M. Miyata, *J. Am. Chem. Soc.*, 2004, **126**, 1764.
- 21 R. E. Melendez, C. V. K. Sharma, M. J. Zaworotko, C. Bauer and R. D. Rogers, *Angew. Chem., Int. Ed. Engl.*, 1996, **35**, 2213.
- 22 K. Biradha, D. Dennis, V. A. MacKinnon, C. V. K. Sharma and M. J. Zaworotko, *J. Am. Chem. Soc.*, 1998, **120**, 11894.
- 23 A. Ranganathan, V. R. Pedireddi, G. Sanjayan, K. N. Ganesh and C. N. R. Rao, *J. Mol. Struct.*, 2000, **522**, 87.
- 24 T. Friščić, A. V. Trask, W. Jones and W. D. S. Motherwell, *Angew. Chem., Int. Ed.*, 2006, **45**, 7546.
- 25 A. J. Cruz-Cabeza, G. M. Day and W. Jones, *Chem.–Eur. J.*, 2009, **15**, 13033.
- 26 J. T. A. Jones, T. Hasell, X. Wu, J. Bacsá, K. E. Jelfs, M. Schmidtman, S. Y. Chong, D. J. Adams, A. Trewin, F. Schiffman, F. Cora, B. Slater, A. Steiner, G. M. Day and A. I. Cooper, *Nature*, 2011, **474**, 367.
- 27 M. D. Ward in *Molecular Networks. Structure and Bonding*. Springer-Verlag Berlin Heidelberg, 2009, Vol. **132**, p. 1–23.
- 28 P. Metrangolo, Y. Carcenac, M. Lahtinen, T. Pilati, K. Rissanen, A. Vij and G. Resnati, *Science*, 2009, **323**, 1461.
- 29 D. J. Plaut, K. T. Holman, A. M. Pivovar and M. D. Ward, *J. Phys. Org. Chem.*, 2000, **13**, 858.
- 30 M. J. Horner, K. T. Holman and M. D. Ward, *Angew. Chem., Int. Ed.*, 2001, **40**, 4045.
- 31 V. A. Russell, C. C. Evans, W. J. Li and M. D. Ward, *Science*, 1997, **276**, 575.
- 32 V. A. Russell, M. C. Etter and M. D. Ward, *J. Am. Chem. Soc.*, 1994, **116**, 1941.
- 33 M. J. Horner, T. K. Holman and M. D. Ward, *J. Am. Chem. Soc.*, 2007, **129**, 14640.
- 34 A. I. Kitaigorodsky *Organic Chemical Crystallography*. Consultants Bureau, New York, 1961.
- 35 (a) A. Kálmán, G. Argay, D. Scharfenberg-Pfeiffer, E. Höhne and B. Ribár, *Acta Crystallogr., Sect. B: Struct. Sci.*, 1991, **47**, 68; (b) A. Kálmán, L. Párkányi and G. Argay, *Acta Crystallogr., Sect. B: Struct. Sci.*, 1993, **49**, 1039; (c) L. Fábián and A. Kálmán, *Acta Crystallogr., Sect. B: Struct. Sci.*, 1999, **55**, 1099.
- 36 D. Cinčić, T. Friščić and W. Jones, *New J. Chem.*, 2008, **32**, 1776.
- 37 D. Cinčić, T. Friščić and W. Jones, *Chem.–Eur. J.*, 2008, **14**, 747.
- 38 D. Cinčić, T. Friščić and W. Jones, *Chem. Mater.*, 2008, **20**, 6623.
- 39 G. R. Desiraju, *Nat. Mater.*, 2002, **1**, 77.
- 40 P. G. Jones and F. Vancea, *CrystEngComm*, 2003, **5**, 303.
- 41 L. Fábián, G. Argay, A. Kálmán and M. Báthori, *Acta Crystallogr., Sect. B: Struct. Sci.*, 2002, **58**, 710.
- 42 A. Kálmán, L. Fábián and G. Argay, *Chem. Commun.*, 2000, 2255.
- 43 A. J. Cruz-Cabeza, G. M. Day, W. D. S. Motherwell and W. Jones, *Cryst. Growth Des.*, 2007, **7**, 100.
- 44 J. Galcera and E. Molins, *Cryst. Growth Des.*, 2009, **9**, 327.

- 
- 45 T. Friščić and W. Jones, *Cryst. Growth Des.*, 2009, **9**, 1621.
- 46 M. B. J. Atkinson, D. K. Bučar, A. N. Sokolov, T. Friščić, C. N. Robinson, M. Y. Bilal, N. G. Sinada, A. Chevannes and L. R. MacGillivray, *Chem. Commun.*, 2008, 5713.
- 47 M. C. Etter, J. C. MacDonald and J. Bernstein, *Acta Crystallogr., Sect. B: Struct. Sci.*, 1990, **46**, 256.
- 48 L. R. Nassimbeni, *Acc. Chem. Res.*, 2003, **36**, 631–637.
- 49 M. J. Frisch, G. W. Trucks, H. B. Schlegel, G. E. Scuseria, M. A. Robb, J. R. Cheeseman, J. A. Montgomery Jr., T. Vreven, K. N. Kudin, J. C. Burant, J. M. Millam, S. S. Iyengar, J. Tomasi, V. Barone, B. Mennucci, M. Cossi, G. Scalmani, N. Rega, G. A. Petersson, H. Nakatsuji, M. Hada, M. Ehara, K. Toyota, R. Fukuda, J. Hasegawa, M. Ishida, T. Nakajima, Y. Honda, O. Kitao, H. Nakai, M. Klene, X. Li, J. E. Knox, H. P. Hratchian, J. B. Cross, V. Bakken, C. Adamo, J. Jaramillo, R. Gomperts, R. E. Stratmann, O. Yazyev, A. J. Austin, R. Cammi, C. Pomelli, J. W. Ochterski, P. Y. Ayala, K. Morokuma, G. A. Voth, P. Salvador, J. J. Dannenberg, V. G. Zakrzewski, S. Dapprich, A. D. Daniels, M. C. Strain, O. Farkas, D. K. Malick, A. D. Rabuck, K. Raghavachari, J. B. Foresman, J. V. Ortiz, Q. Cui, A. G. Baboul, S. Clifford, J. Cioslowski, B. B. Stefanov, G. Liu, A. Liashenko, P. Piskorz, I. Komaromi, R. L. Martin, D. J. Fox, T. Keith, M. A. Al-Laham, C. Y. Peng, A. Nanayakkara, M. Challacombe, P. M. W. Gill, B. Johnson, W. Chen, M. W. Wong, C. Gonzalez, J. A. Pople, *Gaussian 03*, Revision B.03., Gaussian, Inc., Wallingford CT, 2004.
- 50 S. L. Price, M. Leslie, G. W. A. Welch, M. Habgood, L. S. Price, P. G. Karamertzanis and G. M. Day, *Phys. Chem. Chem. Phys.*, 2010, **12**, 8478.